Natural quaternary benzo[c]phenanthridine alkaloids selectively stabilize G-quadruplexes

Petra Jarosova [a], Petr Paroulek [a], Michal Rajecky [a], Veronika Rajecka [a], Eva Taborska [b], Ramon Eritja [c], Anna Aviñó [c], Stefania Mazzini [d], Raimundo Gargallo[e], Petr Taborsky*[a]

[a] Faculty of Science, Masaryk University, Kamenice 5, Brno 62500, Czech Republic

[b] Faculty of Medicine, Masaryk University, Kamenice 5, Brno 62500, Czech Republic

[c] Institute for Advanced Chemistry of Catalonia (IQAC-CSIC), CIBER-BBN, Jordi Girona 18-26, E-08034 Barcelona, Spain.

[d] Department of Food, Environmental and Nutritional Sciences (DEFENS), Section of Chemical and Biomolecular Sciences, University of Milan, Via Celoria 2, Milan 20133, Italy;

[e] Department of Chemical Engineering and Analytical Chemistry, University of Barcelona, Martí i Franquès 1-11, 08028 Barcelona, Spain

Abstract

In this work, the interaction of six natural benzo[c]phenanthridine alkaloids (macarpine, sanguilutine, sanguirubine, chelerythrine, sanguinarine and chelirubine) with parallel and antiparallel G-quadruplex DNA structures was studied. HT22 corresponding to the end of human telomere and the modified promoter oncogenes c-kit21 and Pu22 sequences have been used. Spectroscopically-monitored melting experiments and fluorescence titrations, competitive dialysis and nuclear magnetic resonance spectroscopy were used with this purpose. The results showed that these alkaloids stabilized G-quadruplex structures in terms of increments of T_m values (from 15 to 25 ^oC) with high selectivity over duplexes and unfolded DNA. The mode of binding was mainly by stacking on the terminal G-tetrads with stoichiometries 1:2 (DNA:ligand). The presence of non-specific electrostatics interaction was also observed. Overall, the results pointed to a strong and selective stabilization of G-quadruplex structures by these alkaloids.

Keywords: benzo[c]phenanthridine alkaloids, G-quadruplex, NMR, competitive dialysis, CD.

Introduction

Quaternary benzo[c]phenanthridine alkaloids (QBAs) belong to the group of isoquinoline alkaloids. QBAs are present in plants from families *Fumariaceae*, *Papaveraceae*, *Ranunculaceae* and *Rutaceae*. In addition to relatively common alkaloids such as sanguinarine and chelerythrine, other less common alkaloids such as sanguilutine, macarpine, sanguirubine, chelilutine or chelirubine have been extracted (Figure 1). [1] Some of these have proven

antiproliferative effects on skin melanoma cells.[2] Chelerythrine and sanguinarine, as they are commercially available, have been investigated worldwide and their ability to inhibit some important enzymes in cancer cell division has been demonstrated many times.[3-5] Macarpine, which is found in plants in very small amounts, was first artificially prepared by T. Ishikawa[6]. This alkaloid and its derivatives also show strong cytotoxic effects in cancer cells.[7] In the case of chelirubine and sanguirubine, antimicrobial, anti-parasitic and anticancer effects have been demonstrated.[8, 9] Besides these various biological effects on cells[10], QBAs in iminium form were reported to interact with double stranded DNA (dsDNA),with a relatively weak mode [1, 11] and comparable to that of ethidium bromide[12]. . This interaction leads to change in their fluorescent properties. Because of this change, they could also be used as fluorescent DNA probes.

Other secondary structures of DNA have gained interest in recent years. One of these structures is the G-quadruplex (GQ), which is present in several protoncogenic-DNA promoters and thus participates in processes such as replication, transcription and translation[13, 14]. The building blocks of these structures are the G-tetrads: almost planar arrangements of four guanine bases bonded by eight Hoogsteen hydrogen bonds (Figure 1). The G-quadruplex structure can be formed by the intermolecular association of four DNA molecules, by the dimerization of two molecules that contain two G-tracts, or by the intramolecular folding of a single molecule that contains four G-tracts. The topology of G-quadruplexes may be parallel, antiparallel or hybrid, depending on the spatial orientation of the four G-tracts.

A great interest is observed in the potential of G-quadruplex as anticancer target, being the enzymatic activity inhibited by small ligands which stabilize the G-quadruplex. [Siddiqui et al. Procs 2002, Bucket et al. Yang 2014]

In this work we have studied the ability of several natural alkaloids to stabilize G-quadruplex by interaction with DNA sequences, that have been shown to form homogeneous antiparallel and parallel G-quadruplex structures (Table 1).

The HT22 sequence, 5'-A($G_3T_2A)_3G_3$-3', corresponds to the end of the human telomere and may adopt different G-quadruplex structures depending on the environmental conditions. To date, at least five distinct intramolecular G-quadruplex folding topologies have been reported for natural human telomeric repeats[15, 16], four of which were observed in the presence of K^+ ions[17]. The crystal structure of this sequence in the presence of K^+ formed a parallel intramolecular G-quadruplex[18]. Subsequent studies suggested that the intramolecular G-quadruplex structure observed in the K^+-containing crystal appears unlikely to be the major form in K^+-containing solution. Later, studies have shown that the telomeric sequence can form a mixed (3 parallel + 1 antiparallel) structure in K^+ solution[19]. More recently, another form was observed in K^+ solution, consisting of a two-G-tetrad basket-type core with extensive base stacking interactions in the loops[15]. Very recently, in Na^+ solution[20] an antiparallel (2+2) structure has been observed.

c-kit1 and c-kit2 sequences have been identified within the promoter segment of the human c-kit oncogene, upstream of the transcription initiation site. The 21-mer sequence (5'-$CG_3CG_3CGCGAG_3AG_4$-3') forms polymorphic G-quadruplex structures[21-23] but the mutated sequences (c-kit21T21, Table 1), 5'-$CG_3CG_3CGCGAG_3AG_3$T-3', and c-kit21T12T21, with one G to T mutation at level of 21 and with two G to T mutations at level of 12 and 21 residues, respectively, displays more simple conformations. The G21T mutation restrains the length of the third loop to a

single nucleotide and the fourth G-tract to three guanines. This modification has a significant effect on the biophysical properties, leading to the stabilization of the parallel-stranded topology.[24, 25] The first sequence was used in the present work for CD and fluorescence experiments, the second one for nuclear magnetic resonance (NMR) spectroscopy.

Another important oncogene is c-myc, the overexpression of which is the cause of a wide range of genetic tumors. Pu22 is a 22-mer sequence mainly responsible for the c-myc transcriptional activity. Pu22-14T23T is the same sequence with two G to T mutations at position 14 and 23. It adopts the single predominant intramolecular parallel G-Quadruplex conformation under K^+ physiological concentration, and thus shows better resolved NMR spectra. [Ambrus et al. Biochemistry 2015]. Recently it has been reported that Pu22-14T23T gives the same interactions with ligands as wild type Pu22. [Scaglioni et al. BBA, 2016; Dai et al. JACS 2011]

In this work, the interaction of six natural benzo[c]phenanthridine alkaloids (macarpine, sanguilutine, sanguirubine, chelerythrine, sanguinarine and chelirubine) with G-quadruplex DNA structures formed by HT22,c-kit21T21, c-kit21T12T21 and Pu22T14T23 sequences was studied. Spectroscopically-monitored melting experiments and fluorescence titrations, competitive dialysis and nuclear magnetic resonance spectroscopy were used with this purpose.

Materials and Methods

Chemicals

Alkaloids were extracted from plant material in Department of Biochemistry, Faculty of Science, Masaryk University (Brno, Czech Rep.). Some of the oligonucleotides used in this work (Table 1) were purchased as dry samples from Thermo Fisher Scientific (USA) at HPLC grade. In other cases, DNA synthesis was performed on an Applied Biosystems DNA/RNA 3400 synthesizer by solid-phase 2-cyanoethylphosphoroamidite chemistry. DNAs were desalted in a Sephadex (NAP-10) G25 column and passed through a DOWEX(Na^+) resin to exchange triethylammonium to sodium cations. In all cases, DNAs were diluted in re-distilled water with Trizma® base (10 mM) and EDTA (0.1 mM) buffer (pH = 8) to stabilize them during storing. Other chemicals such Trizma® base ($C_4H_{11}NO_3$, p.a.) and EDTA (p.a.) were obtained from Sigma-Aldrich (USA). Basic chemicals such as KH_2PO_4, KCl, NaOH and KOH (all p.a. grade) were purchased from Lach-Ner (Czech Rep.).

Instruments

Absorbance spectra were recorded on an Agilent 8453 diode array spectrophotometer (Agilent Technologies; Waldbronn, Germany). Temperature was controlled by means of an Agilent 89090A Peltier device (Agilent Technologies). CD spectra were recorded on a Jasco J-810 spectropolarimeter equipped with a JULABO F-25-HD temperature control unit (Seelbach, Alemania). Fluorescence spectra were measured with an Aminco-Bowman Series 2 spectrofluorimeter (Thermo-Spectronic, USA), equipped with xenon lamp. Temperature was controlled by means of a water bath. Excitation wavelength was depending on QBA used for titration. It differs from 330 to 350 nm. Emission wavelength for complex QBA:DNA is 600 nm. In all spectroscopic studies, Hellma quartz cells (10 mm path length, and 350, 1500 or 3000 µl volume) were used. The NMR spectra were recorded on a Bruker AV600 spectrometer operating at a frequency of 600.10 MHz, equipped with a 5 mm TXI inverse probe and *z* -axis

gradients. The ^{1}H spectra were referenced to external DSS (2,2-dimethyl-2-silapentane-5-sulfonate sodium salt) set at 0.00 ppm.

Melting experiments

In typical melting experiment, DNA (final concentration in cuvette 2 μM) was mixed with QBA (4 μM) together with phosphate buffer (10 mM) and KCl (5 mM). The concentration of KCl was set to 5 mM instead of the most usual 100 or 150 mM concentration in order to reduce the high thermal stability of GQ structures. In this way, the potential stabilization of the GQ by the presence of QBA in terms of ΔT_m could be determined accurately. The sample was heated (96°C) and then allowed to cool slowly. After several hours, the sample in cuvette was placed to instrument (Agilent 8453 UV-Vis or Jasco J815 CD spectrometers). Stirred sample was heated to 96°C and cooled down during measurement at a rate of 0.5°C·min^{-1}. Sample was measured also during heating process starting from 20 °C to 96 °C in the same rate. The absence of hysteresis was checked for some of the QBA:DNA mixtures. Melting temperatures (T_m) were determined as described elsewhere[26] using home-made routines written in Matlab® code.

Fluorescence experiments Fluorescence measurements were performed to determine binding stoichiometries and overall formation constants according to equation 1:

$$DNA + nLigand \rightleftharpoons DNA \cdot ligand_n \qquad \beta = \frac{[DNA \cdot ligand_n]}{[DNA] \cdot [ligand]^n} \quad \text{Equation 1}$$

Stability constants were determined from fluorescence-monitored titrations of QBAs by GQ at 25°C. In all experiments, the concentration of QBA was kept constant (3 μM) whereas the concentration of the considered GQ was increased.

Binding data analysis was done with the OPIUM program [Petra: include reference].

Alternatively, the Job method was used to determine the binding stoichiometry of the QBA:GQ interaction complex. In this method, the total molar concentration of the two molecules was kept constant, whereas the molar fraction was varied. The total concentration of QBA and GQ was 3 μM. The stoichiometry of the QBA:DNA interaction complex was estimated from the intersection of two lines fitting those points measured at lowest and highest molar fractions.

Competitive dialysis studies

A 100 μl of a 50 μM DNA in 6mM sodium phosphate + 1mM EDTA buffer (pH 7.0) with 10 mM potassium chloride was introduced into a separated dialysis unit and a blank sample containing only buffer. All dialysis units were allowed to equilibrate during 24 h at room temperature in a beaker containing the 1 μM solution of the appropriate QBA. At the end of the dialysis experiment, the amount of QBA bound to the DNA was quantified by measuring the fluorescence spectra. ANNA: CHECK THIS PARAGRAPH

Nuclear Magnetic Resonance

The NMR samples of Pu22-T14T23 and c-kit21T12T21 (Table 1) were prepared at concentration 0.34 mM and 0.42 mM. Pu22-T14T23 was dissolved in 25 mM KH_2PO_4, 70 mM KCl, pH 6.9 and ckit21T12T21 was dissolved in 5mM KH_2PO_4, 20 mM KCl, pH 6.9. In these salts condition ckit21T12T21 is present as a monomeric form (Form I).[23] The DNA samples were heated to 85°C for 1 min and then cooled at room temperature overnight. Stock solution of QBAs were prepared in DMSO-*d6* because the sanguilutine was poorly soluble in water.

^{1}H NMR titrations were performed at 25°C by adding increasing amounts of the QBA to the DNA at different ratio R=[QBA]/[DNA] and by adding the DNA to a QBA solution in the same experimental conditions.

The protons in the complexes were assigned by using NOESY and TOCSY experiments. Phase sensitive NOESY spectra were acquired at 25 °C and 35 °C. The best results were obtained at 25 °C, in TPPI mode, with 2048 x 1024 complex FIDs. Mixing times ranged from 100 ms to 300 ms. TOCSY spectra were acquired with the use of a MLEV-17 spin-lock pulse (60 ms total duration). All spectra were transformed and weighted with a 90° shifted sine-bell squared function to 4K x 4K real data points. Proton resonance assignments of GG21-T12T21 and Pu22-T14T23 free and complexed were performed on the basis of previous assignments.[23,27] The chemical shift values of the complex of chelerythrine with ckit21T12T21 are reported in Table 2. The chemical shift values of the complexes of Pu22-T14T23 with sanguilutine and chelerythrine are reported in Table S1 and Table 3 respectively. The assignment of the resonances of sanguilutine and chelerythrine in the complexes are reported in Tables S2. Some aromatic protons of chelerythrine and sanguilutine lie in a crowded region of the oligonucleotide signals and thus could not be assigned. Pseudo two-dimensional DOSY experiments were acquired using the pulse-program "stebpgp1s", diffusion delay: 0.24–0.36 s; gradient pulse: 1.5 ms; number of increments: 64. Raw data were processed using the standard DOSY software present in the Bruker library (TOPSPIN v. 1.3).

Results and discussion

Effect of QBAs on G-quadruplex structure by CD and fluorescence experiments

First, the overall G-quadruplex structures formed by the HT22 and ckit21T21 sequences at the experimental conditions were identified by means of CD spectroscopy (Figure S1). The shape and position of the bands in the CD spectra reflected the overall antiparallel or parallel nature of the GQ structure. Hence, a positive band around 285 nm indicated the predominance of the antiparallel structure in the case of HT22 sequence, and a negative band around 240 nm were indications of a parallel structure in the case of the ckit21T21 sequence. In general, the addition of QBA to both HT and ckit21T21 GQ structures did not affect dramatically to the overall GQ structure.

Thermal stabilization

Melting experiments were made in order to observe any positive contribution of QBAs to the thermal stability of GQ structures. Table 4 summarizes the determined T_m values in the presence of QBAs.

The melting experiments with antiparallel structure HT22 were monitored either with UV-Vis or CD spectroscopies. The determined T_m values in both cases were very similar (within 0.5°C). Melting temperature of HT22 was found to be 51.0°C (Figure 2). Practically no changes between melting temperatures calculated from data obtained during cooling or heating the studied systems were observed (Figure S2), which ruled out the presence of hysteresis. Except for macarpine, all other QBAs produced a dramatic stabilization of this GQ structure. The highest T_m value in case of HT22 was observed for sanguinarine (ΔT_m = 18,1 °C) and the most conspicuous shift in case of ckit21T21 was observed for sanguiltuine (ΔT_m = 22,4 °C).

The melting experiments on parallel structure c-kit21T21 were exclusively made by CD spectrometry because of low absorbance changes at 295 nm during measurements. The T_m value of c-kit21T21 was found to be 50.0°C. Addition of macarpine slightly increased the T_m value to 56°C. The weaker stabilization induced by this QBA could be due to

steric effects related with the additional –O-CH_3 group at position R6. All the other alkaloids, which do not include this group, shifted the T_m to values higher than 65°C. In case of chelirubine, the ΔT_m was around 24.5°C. To our knowledge, this is one of the highest observed differences in melting values for parallel GQ structure.[2930, 3031] TMPyP4 stabilizes telomeric DNA about 1 – 13°C less than selected alkaloids at the same concentration ratio.[3132, 3233]

The observed ΔT_m values may be qualitatively correlated with the presence and nature of substituents in the benzo[c]phenanthridine skeleton of the considered QBAs (Figure 1). The ligands that shift the most the T_m values of HT22 GQ are those showing an H atom at R5 position, and –O-CH_2-O- group between R1 and R2. The substitution on R4, R6, or R3 does not have any significant influence on ΔT_m. The ligands showing significant T_m increase of c-kit21T21 are those having an H atom at R6, and no –OCH_2-O– group between R3 and R4. The substitution at R2, R5 and R1 has little influence on the stabilization.

Selectivity

At this point, it is necessary to mark that melting experiments with dsDNAs and QBAs did not show any significant increase of melting temperature (ΔT_m < 2°C) (Figure 2b). Therefore, QBAs appeared as a potential selective group of ligands to bind GQ structures.

In order to gain more information about the selectivity of QBAs for DNA structures or sequences, competitive dialysis experiments were performed using a set of different DNA sequences (Table 1) representing several nucleic acid structures.[23, 3334, 3435] T20 was used as model for an unfolded DNA sequence. As models of dsDNA, the self-complementary sequences Dickerson-Drew dodecamer and a 26-mer hairpin (ds26) were used. Finally, bcl-2, an additional DNA sequence known to form a hybrid antiparallel-parallel GQ structure was also selected[536]. Competitive dialysis experiments showed clear differences on the affinity of QBAs to a different DNA structures (Figure 3 and Table S3). In general, all QBAs showed higher affinities for GQ structures than for dsDNA or for the unfolded sequence. Sanguinarine and sanguilutine showed the highest selectivity, whereas chelirubine showed the lowest one.

Determination of DNA:ligand stoichiometry

The interaction of GQ with the QBAs causes an increase of their intrinsic fluorescence that can be used to determine stoichiometries and to calculate binding constants (Figure 4) by means of mole-ratio experiments. In these, the concentration of QBA was kept constant (3 μM) whereas the concentration of the considered GQ was increased along the experiment. At the temperature of the experiment, 25°C, GQ structures are completely folded as the corresponding T_m values are higher than 50 °C. On the other hand, the emission was measured in a region (500 – 600 nm) where the potential inner effect filter due to absorption of the titrant (around 260- 300 nm) cannot be produced.

Figure 4a shows the titration of MA with HT22. The titration curve showed the typical sharp initial slope of intensity with increase of GQ concentration indicating a strong interaction. At higher concentration of GQ, instead of the constant fluorescence intensity, the signal was continuously increasing. This fact would indicate additional non-specific interaction between QBAs and GQ, which could be related to a weak electrostatic interaction between positively charged QBA and the anionic phosphate backbone. From titration curves binding stoichiometry and stability constants were estimated (Table 4). The non-specific interaction was considered in the model and the best

fitting models were found to have (GQ:QBA) stoichiometry 1:3 or 1:4. PETRA/PETR: DO WE HAVE ANY VALUE OF THE LACK OF FIT FOR EACH CALCULATION? HOW COULD WE QUANTIFY THE NON-SPECIFIC INTERACTION? COULD WE SAY THAT 1:3 INCLUDES SPECIFIC AND NON-SPECIFIC INTERACTION? Additional experiments based on Job's method provided similar values of stoichiometry. PETRA/PETER: WE SHOULD INCLUDE SEVERAL EXAMPLES AS SUPPLEMENTARY MATERIAL

The 1:3 stoichiometry was the best fit for both studied GQ structures with almost all alkaloids. At neutral pH QBAs are mostly in iminium (positively charged) form as their pK_{R+} values lie between 7.7 and 9[37]. As previously reported, QBAs in iminium form interact with dsDNA forming highly luminescent complexes.[38] Although there is no clear evidence for the mechanism of interaction with dsDNA, it is supposed that planar positively charged alkaloids are intercalated between base pairs of DNA and due to this incorporation, the luminescence is enhanced (except for sanguinarine). A similar enhancement of the luminescence emission was observed also for mixtures of QBAs with GQ. However, the intercalation mechanism does not seem a very plausible possibility because of insufficient space for the ligands between tetrads of GQ which, moreover, are probably occupied by cations [39,40]. In this sense, the stoichiometries determined in this work are far from the 1:1 (GQ:QBA) stoichiometry described by Bhadra[29] for sanguinarine, coralyne, palmatine and berberine with 5'-$AG_3(T_2AG_3)_3$-3'. However, it should be taken into account that the experimental conditions were different and these could not only affect to the GQ structure (which was an hybrid parallel/antiparallel in that work) but also to the non-specific interactions.

Xiong et al.[40] described three possible binding modes of heterocyclic alkaloids: stacking on the top or bottom G-quartets, groove binding and loop binding. Although it is not possible to assign exact binding mode of interaction from spectroscopic experiments, it seems that there exist ~3 binding sites occupied by molecules of QBA with similar energetic level[42,432]. Enhancement of fluorescence at 620 nm (similar to intercalation) would be explained by stacking (π-π stacking interaction) of QBA to structure of GQ resulting in low fluorescence quenching by water molecules or other quenchers present in solvent. The stacking interaction is also reported by other authors [43,44] and it is in agreement with observation provided by Shu et al.[42] and Bhadra et al.[28] for sanguinarine.

Interaction of chelerythrine with c-kit21T12T21 sequence and of sanguilutine and chelerythrine with Pu22-T14T23 sequence

NMR experiments were used to study the mode of binding of these alkaloids with the G-quadruplex structures found in the c-myc and c-kit 2 promoter oncogenes.

The addition of chelerythrine to c-kit21T12T21 solution even at low ratio R=[ligand]/[DNA]=0.5/1.0 produced an upfield shift and a generalized broadening of H1 imino protons. The signals still remain broad till the ratio R=3.0 was reached and a precipitate is formed (Figure 5). The assignment of the protons involved in the tetrads for the complexes and for the free nucleotides was performed by a combined used of a) the inter-residue NOE interactions between H1 imino protons (Table S4), b) the titration experiments and c) the inter-residue NOE connectivities between the H1 imino and aromatic H8 of guanine residues.

A large change in the chemical shifts of the H1 imino protons ($\Delta\delta \geq 0.80$ ppm) was observed both for the H1 imino protons belonging to outer G-tetrads and for the internal one ($\Delta\delta \geq 0.40$ ppm) (Table 2). A number of NOE contacts

were found: the aromatic proton H6 of chelerytrine with H1 imino protons of G18, G7 and G19, the NCH_3 protons with G20, and the 8-ethylene-dioxy with G18, suggesting strong interactions of chelerythrine with the oligonucleotide (Table 5). The generalized line broadening of all the signals and the presence of the NOE interactions either with the external and internal tetrads suggest the presence of multiple species in solution with the ligand positioned in different binding sites in chemical exchange. Also the protons of the chelerythrine in the complex are broad, indicating a certain mobility inside the binding sites.

In order to better clarify the mode of binding of these alkaloids with the parallel G-quadruplex structure and to extend our investigation to the sequence responsible for the c-myc transcription activity we performed the NMR experiments with the Pu22-T14T23 sequence.

The titration with chelerythrine and sanguilutine induced, even at low R=[ligand]/[DNA] ratio, a broadening of all the signals of DNA and of the ligand. At R ≥ 1.5 a new set of imino protons signals appeared at up-field shift, and the signals sharpened at R=2.0 (Figure 6). This suggested the formation of a defined complex with two ligand molecules interacting with the G-Quadruplex structure. A further addition of ligands to Pu22-T14T23 caused only small changes in the H1 imino protons until the R = 3.0 was reached.

The analysis of the spectra at R=3.0 was performed starting from the attribution of the three tetrads by inter-residue NOE connectivities between the H1 imino and the aromatic protons H8 of guanine residues (following the procedure used for the study of other ligands. [Scaglioni 2016; Musso 2018].The results reported in Table S5 show that the quadruplex structure is conserved. Also for these complexes a significant shielding was observed for the H1 imino protons of the internal tetrad ($\Delta\delta$ = -0.30/-0.60 ppm) although lower than the values of the external tetrads ($\Delta\delta \geq$ -0.60 ppm). In particular, it is relevant the $\Delta\delta$ =-1.36 ppm observed for the G16H1 of the chelerythrine complex (Table 3 and Table S1).

Sanguilutine showed NOE contacts of H6 with G22 H1. Other NOEs were found between some aromatic protons and H1 imino protons of G9, G18 and G22 belonging to the 3'-end tetrad. The methyl signal confirms the contacts to all these units and to G11 H1 belonging to the 5'-end tetrad. Due to the low solubility of the sanguilutine, the identification of all the aromatic protons of the ligand was difficult. The NMR spectra of chelerythrine complex instead are of better quality and all the proton signals of the ligand were identified. NOEs were found between the N-methyl and the aromatic protons H4 and H6 of the ligand with the H1 imino protons of G7 , G11 and G16 units at 5'-end. The same protons of the ligand also show NOE contacts with units at 3'-end, *i.e*. G9, G22, G18 and/or G13 (Table 6)(figure 7). These results gave evidence of the location of chelerythrine over both the outer G-quartets.

DOSY experiment, performed on the complex with chelerythrine, showed a diffusion coefficient indicating that the stoichiometry of the complex may be more than two ligands for G-quadruplex and excludes a higher aggregation of the nucleotide. The significant upfield chemical shifts of the imino protons belonging to the internal tetrad are difficult to be explained but they can suggest an interaction also at the level of this tetrad.

Conclusions

The interaction between G-quadruplex DNA structure and six plant benzo[c]phenanthridine alkaloids appears selective over the duplex and unfolded DNA structure. Although these alkaloids have similar structure, they exhibit different contribution to stabilization of G-quadruplex structures as demonstrated with melting experiments. The ligands that mostly shift the T_m of HT22 are those showing an H atom at R5 position, and $–O-CH_2-O-$ group between R1 and R2. The fluorescence experiments show that the stoichiometry can reach GQ:QBSAs 1:3/1:4 values and the Ka……..

Sanguinarine and chelerythrine in particular were found to be good stabilizers of anti-parallel and parallel structures as those present in the segment of human telomeric and in the modified 21-mer of c-kit2 sequences.

The NOESY experiments, performed with c-kit21T12T21 and Pu22T14T23 sequences, show that sanguilutine and chelerythrine have NOEs contacts with units at 3'and 5' end, with two molecules being located respectively over the outer tetrads.

The possibility that the ligand molecules may interact also at the level of the internal tetrad is suggested by the strong shelding of the imino protons signals of these units. This appears more probable for the complex with c-kit21T21 sequence, where the ligand positioned in different binding sites appears in chemical exchange.

Overall, these results suggest the potential use of these minor, non-commercial QBAs as G-quadruplex stabilizers *in vivo*, or for the development of analytical methods based on fluorescence spectroscopy.

Aknowledgments

Funding from Spanish government (CTQ2015-66254-C2-2-P and CTQ2017-84415-R) and recognition from the Autonomous Catalan government (2017SGR114) are acknowledged. This work was also supported by the project KONTAKT II LH12176 from Ministry of Education, Youth and Sports of the Czech Republic. Part of the work was carried out with the support of Biomolecular Interactions and Crystallization Core facility of CEITEC – Central European Institute of Technology, ID number CZ.1.05/1.1.00/02.0068, financed from European Regional Development Fund.

Figure and table legends

Table 1. DNA sequences used in this work. PETRA: The column "Reference" should be filled with numbers, as in the main text – I will do it after all corrections ☺

Code	Sequence (5' → 3')	Proposed structure	Reference
HT22	$A(GGGTTA)_3GGG$	Antiparallel G-quadruplex	Lim et al. NAR 2009
c-kit21T21	CGGGCGGGCGCGAGGGAGGG**T**	Parallel G-quadruplex	Fernando, 2006
T20	T_{20}	Unfolded strand	--
ds26	GAAGGAGGAGATTTTTCTCCTCCTTC	Duplex hairpin	Jaumot, J.; Aviñó, A.; Eritja, R.; Tauler, R.; Gargallo, R. Journal of Biomolecular Structure & Dynamics, 2003, 21, 267 - 278
Dickerson	CGCGAATTCGCG	Duplex	
bcl-2	CGGGCGCGGGAGGAAGGGGGCGGG	Hybrid G-quadruplex	Dai, JACS 2006, 128, 1096
$(GC)_6$	GCGCGCGCGCGC	Duplex	
c- kit21T12T21	CGGGCGGGCGC**T**AGGGAGGG**T**	Parallel G-quadruplex	Kuryavyii et al.
Pu22-T14T23	TGAGGGTGGG**T**AGGGTGGG**T**AA	Parallel G-quadruplex	Dai et al. 2011

Table 2. ^{1}H chemical shift values for the complex of chelerythrine with c-kit21T12T21.[a]

	$H1/H2/H5/CH_3$	$\Delta\delta$[b]	H6/H8	$\Delta\delta$[b]
C1	6.08	+0.53	7.55	+0.05
G2	11.15	-0.81	8.03	-0.17
G3	10.88	-0.42	7.69	-0.09
G4	10.42	-0.73	7.70	-0.05
C5	6.22	+0.02	7.81	-0.23
G6	n.d.	-	n.d.	-
G7	11.07	-0.51	7.84	-0.18
G8	10.48	-0.83	7.76	-0.03
C9	6.20	+0.10	7.62	0.00
G10	n.d.	-	8.03	+0.04
C11	6.10	+0.04	7.94	+0.04
T12	1.88	-0.02	7.50	-0.10
A13	n.d.	-	8.28	+0.18
G14	11.10	-0.84	n.d.	-
G15	10.78	-0.40	7.68	-0.19
G16	10.25	-0.79	7.69	-0.09

A17	n.d.	-	8.56	+0.03
G18	10.69	-1.13	n.d.	-
G19	11.02	-0.50	7.77	-0.32
G20	10.45	-0.80	7.73	+0.03
T21	n.d.	-	n.d.	-

[a] Measured at 25°C in ppm (δ) from external DSS. Solvent H_2O-D_2O (90:10 v/v), 5 mM phosphate buffer, 20 mM KCl, pH 6.9, R = 3. [b] $\Delta\delta = \delta_{bound} - \delta_{free}$

Table 3. [1] H chemical shift values for the complex of chelerythrine with Pu22-T14T23.[a]

	H1/H2/Me	Δδ[b]	H6/H8	Δδ[b]	H1'	Δδ[b]
T4	n.d.	-	n.d.	-	n.d.	-
G5	n.d.	-	n.d.	-	n.d.	-
A6	n.d.	-	n.d.	-	n.d.	-
G7	11.10	- 0.66	8.02	0.00	6.03	-0.03
G8	10.72	- 0.50	7.60	- 0.15	6.03	-0.10
G9	10.09	- 0.56	7.63	- 0.12	n.d.	-
T10	1.95	-0.04	7.68	-0.14	6.28	-0.24
G11	10.95	-0.75	n.d.	-	n.d.	-
G12	10.84	- 0.66	7.63	- 0.27	n.d.	-
G13	10.52	- 0.53	7.72	- 0.14	n.d.	-
T14	1.89	-0.03	7.58	-0.07	6.25	+0.02
A15	8.35	-0.18	8.55	-0.02	6.64	-0.04
G16	10.63	- 1.36	8.18	+0.07	6.22	+0.05
G17	10.92	- 0.33	7.82	+0.02	n.d.	-
G18	10.52	- 0.50	7.60	- 0.18	6.03	-0.39
T19	2.00	+0.01	7.89	+0.03	6.54	+0.02
G20	10.92	- 0.36	n.d.	-	n.d.	-
G21	10.98	- 0.39	7.91	0.00	5.80	-0.24
G22	10.28	- 0.76	7.79	+0.18	6.00	-0.14
T23	1.45	- 0.03	7.03	- 0.11	5.63	- 0.27
A24	n.d.	-	7.93	+0.16	5.68	- 0.07
A25	n.d.	-	7.33	+0.03	5.40	-0.20

[a,b] See footnotes (a) and (b) of **Table 2**.

Table 4. GQ stabilization by QBAs in melting and binding experiments. The experimental conditions of melting studies were 2 μM GQ, 4 μM QBA, 10 mM phosphate buffer, 5 mM KCl, pH 7.0. In the case of binding studies, the experimental conditions were 3 μM QBA, 10 mM phosphate buffer, 5 mM KCl, pH 7.0, 25 °C. GQ concentration varied from 0 to 10 μM. T_m values were determined from two replicates. In all cases, incertitude values are below 1 °C. Figures written in italics are only estimated values because of high experimental error.

GQ	QBA	T_m [°C]	ΔT_m [°C]	Proposed stoichiometry	Logarithm of overall formation constant β (standard deviation)
HT22	no alkaloid	51.0	-	-	-
	Macarpine (MA)	50.1	-0.9	1:5	31.3 (0.1)
	Chelirubine (CHR)	64.6	13.6	1:4	24.5 (0.2)
	Sanguinarine (SG)	69.1	18.1	*1:3*	*~ 16*
	Chelerythrine (CHE)	63.3	12.3	1:3	17.1 (0.1)
	Sanguirubine (SR)	62.2	11.2	1:3	19.3 (0.1)
	Sanguilutine (SL)	57.6	6.6	1:3	19.1 (0.1)
c-kit21T21	no alkaloid	50.0	-	-	-
	Macarpine (MA)	56.3	6.3	1:3	17.6 (0.1)
	Chelirubine (CHR)	74.5	24.5	1:3	17.3 (0.1)
	Sanguinarine (SG)	65.5	15.5	*1:4*	*~ 22*
	Chelerythrine (CHE)	70.7	20.7	*1:3*	*~ 15*
	Sanguirubine (SR)	70.8	20.8	1:4	23.9 (0.1)
	Sanguilutine (SL)	72.4	22.4	1:3	17.9 (0.1)

Table 5. Inter-molecular NOE in the complex of chelerythrine with c-kit21T12T21. Experimental data acquired at 25°C in H_2O-D_2O (90:10 v/v), 5 mM phosphate buffer, 20 mM KCl, pH 6.9.

Ligand	c-kit21TT12T21
H6	G7H1
H6	G18H1
H6	G19H1
O-CH_2-O	G18H1
NCH_3	G20H1

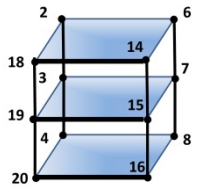

Table 6. Inter-molecular NOE in the complex of chelerythrine with Pu22-T14T23. Experimental data acquired at 25°C in H_2O-D_2O (90:10 v/v), 25 mM phosphate buffer, 70 mM KCl, pH 6.9.

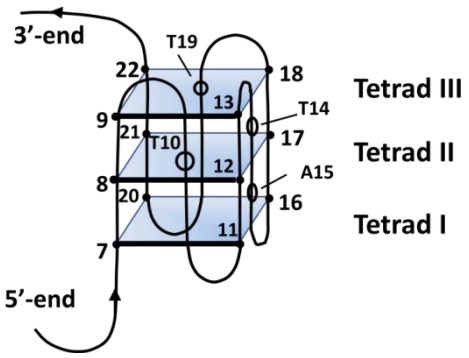

5'-end binding site	
Ligand	Pu22
H4	G11H1
H6	G11H1
H6	G7H1
H6	G16H1
NCH_3	G7H1
NCH_3	G16H1
O-CH2-O	G16H1
3'-end binding site	
H6	G13/G18H1[a]
H4	G22H1
H4	G13/G18H1[a]
NCH_3	G9H1
NCH_3	G13/G18H1[a]
NCH_3	G22H1

[a] The two signals are overlapped

Figure 1. General structure of QBAs and G-quadruplex. (a) General formula of QBAs and acid-base equilibria. (b) Nomenclature and substitutions of the QBAs studied in this work. (c) Planar arrangement of four guanine bases in a G-tetrad. (d) Three different topologies of G-quadruplex structures depending on the spatial arrangement of G-tracts.

a

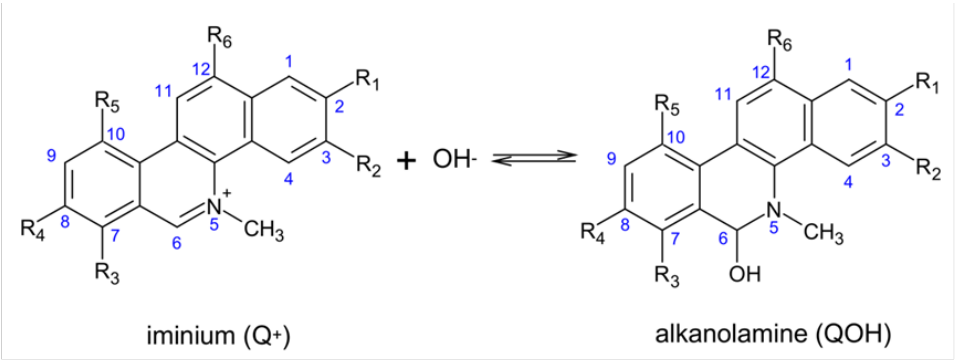

b

	R_1	R_2	R_3	R_4	R_5	R_6
Macarpine (MA)	$-OCH_2O-$		$-OCH_2O-$		$-OCH_3$	$-OCH_3$
Chelirubine (CHR)	$-OCH_2O-$		$-OCH_2O-$		$-OCH_3$	-H
Sanguinarine (SG)	$-OCH_2O-$		$-OCH_2O-$		-H	-H
Chelerythrine (CHE)	$-OCH_2O-$		$-OCH_3$	$-OCH_3$	-H	-H
Sanguirubine (SR)	$-OCH_3$	$-OCH_3$	$-OCH_2O-$		$-OCH_3$	-H
Sanguilutine (SL)	$-OCH_3$	$-OCH_3$	$-OCH_3$	$-OCH_3$	$-OCH_3$	-H

c

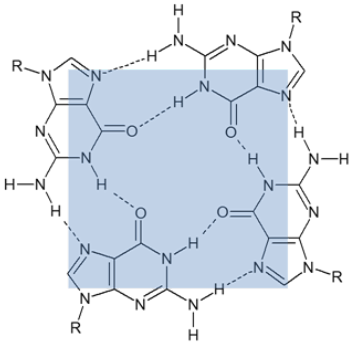

d

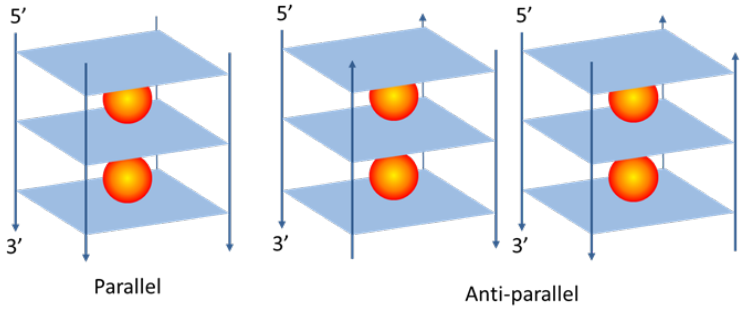

Figure 2. Melting experiments. (a) Normalized melting curves of c-kit21T21 (black) with macarpine (blue) and chelirubine (red). (b) Normalized melting curves of $(GC)_6$ dsDNA (black) with macarpine (blue) and chelirubine (red). In all cases, C_{DNA} = 2 μM, C_{QBA} = 4 μM, 10 mM phosphate buffer, 5 mM KCl, pH 7.0. Petr Paroulek does not have the spectra or "fraction" data in materials I have…. Still looking for it in old computer in office etc….

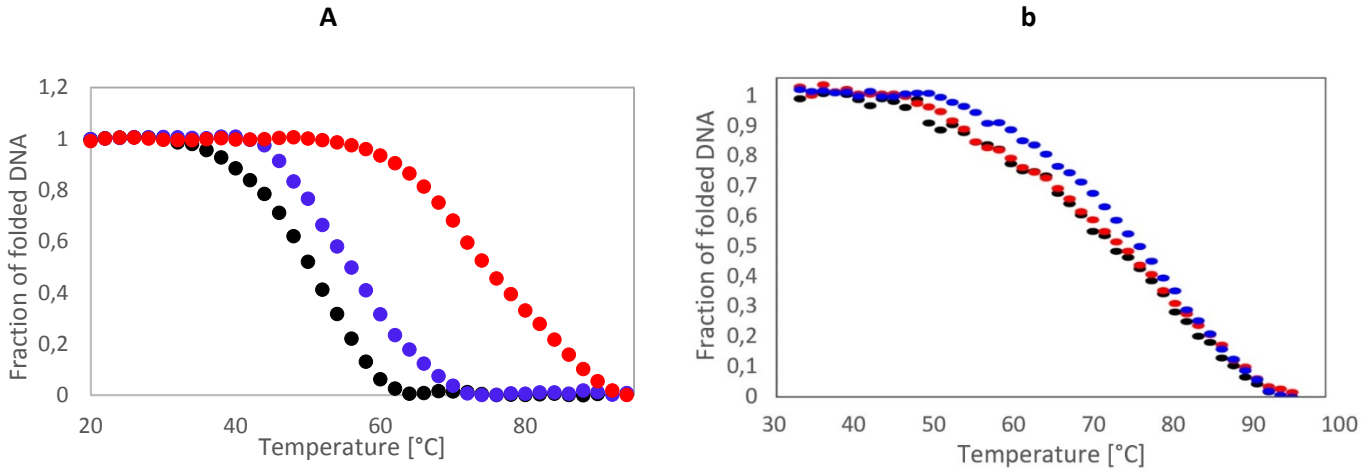

Figure 3. Competitive dialysis assays. Experimental conditions are explained in the text. The amount of ligand bound to each DNA structure is shown as a bar graph. The whiskers indicate an incertitude equal to 10 %.

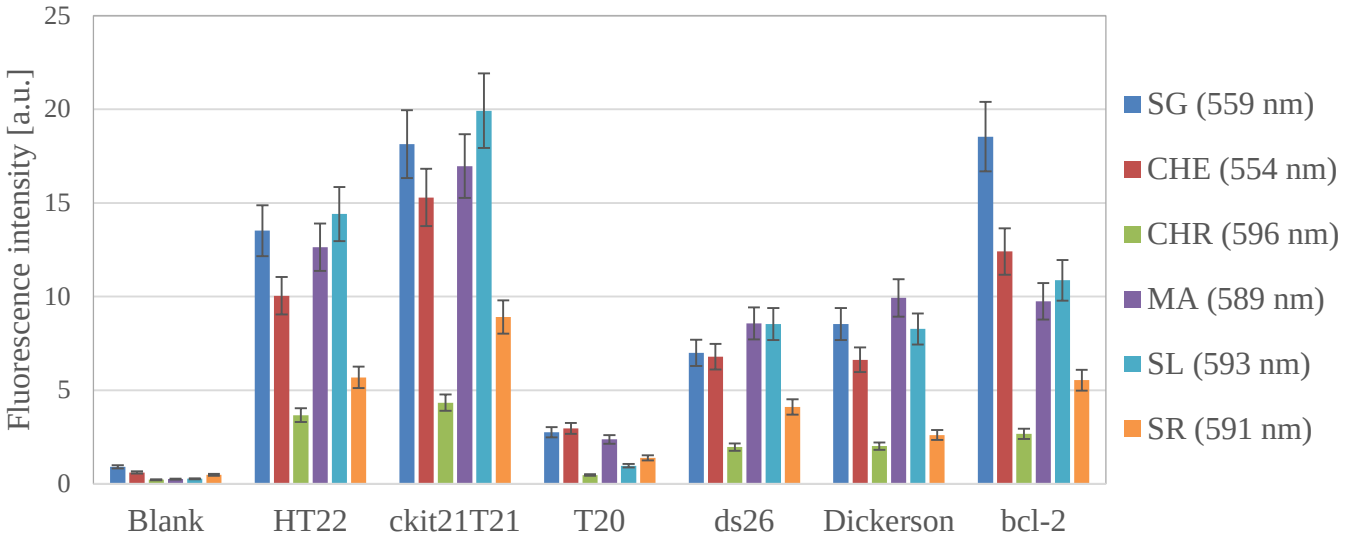

Figure 4. Spectrofluorimetrically-monitored binding studies. (a) Fluorescence spectra recorded along the titration of MA (3 µM) with HT22. Other experimental conditions were 10 mM phosphate buffer, 5 mM KCl, 25 ^{o}C. (b) corrected fluorescence at 600 nm for the titration of MA with HT22. Symbols denote non-specific interaction correction (triangles), non-specific interactions (squares), and corrected signal (circles).

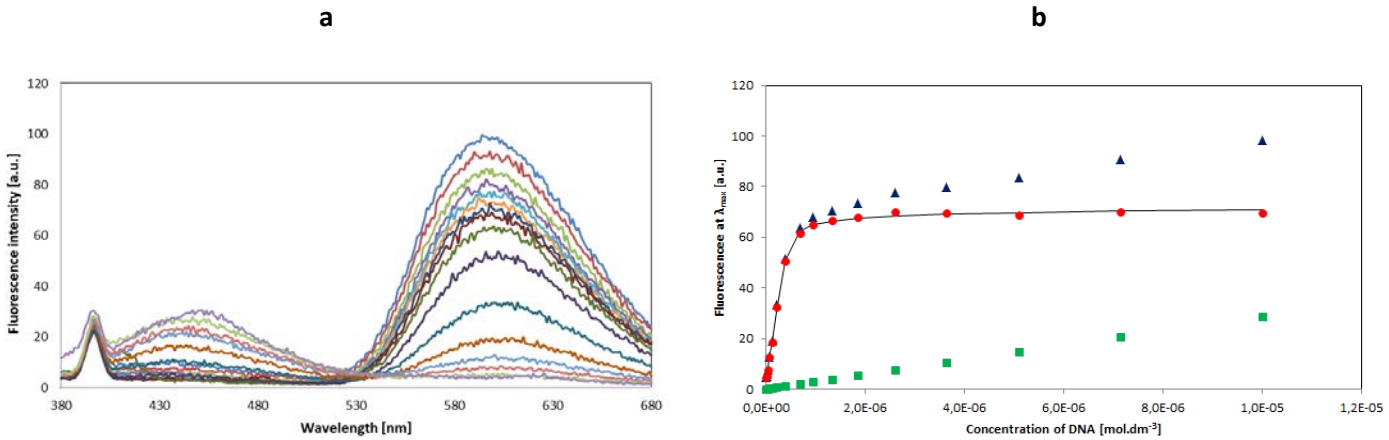

Figure 5. Imino proton region of the 1D NMR titration spectra of c-kit21T12T21 with chelerythrine. Experimental conditions were: 25 °C, H_2O/D_20 (9:1), 25 mM KH_2PO_4, 70 mM KCl, pH 6.9, at different R =[ligand]/[DNA] ratios.

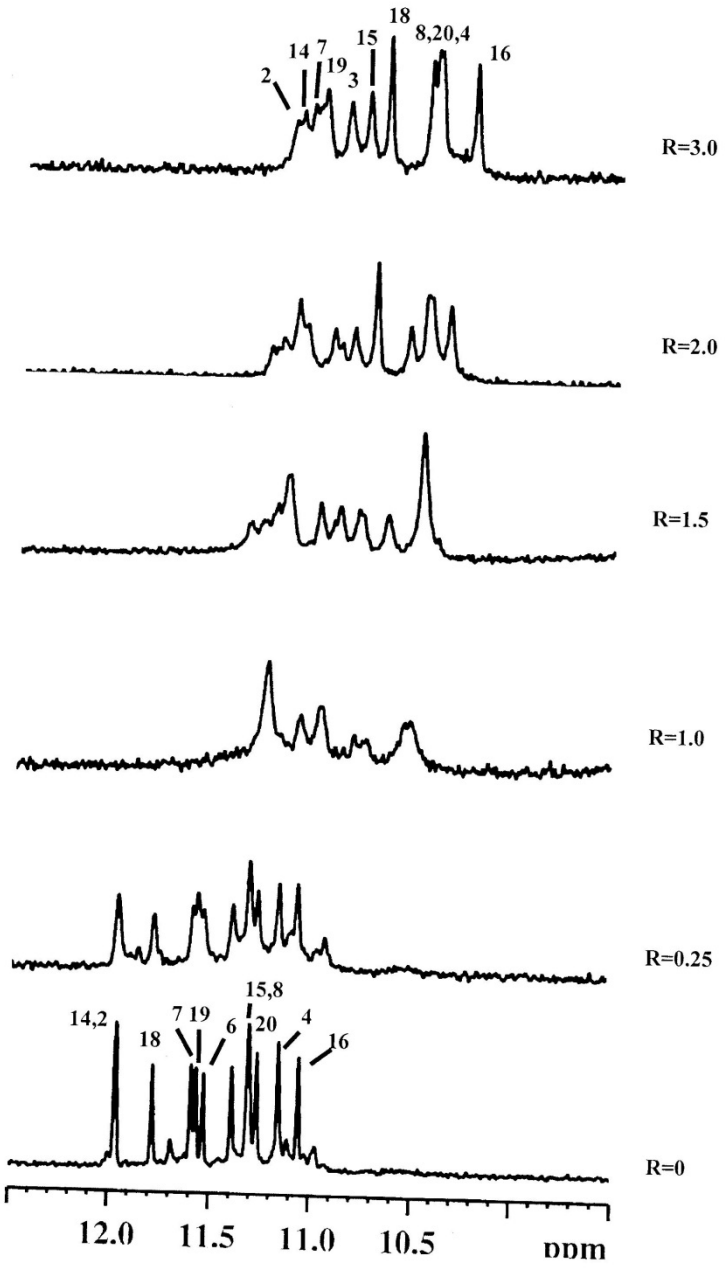

Figure 6. Imino proton region of the 1D NMR titration spectra of Pu22-T14T23 with (a) sanguilutine and (b) chelerythrine. Experimental conditions were: 25 °C, H_2O/D_20 (9:1), 25 mM KH_2PO_4, 70 mM KCl, pH 6.9, at different R =[ligand]/[DNA] ratios.

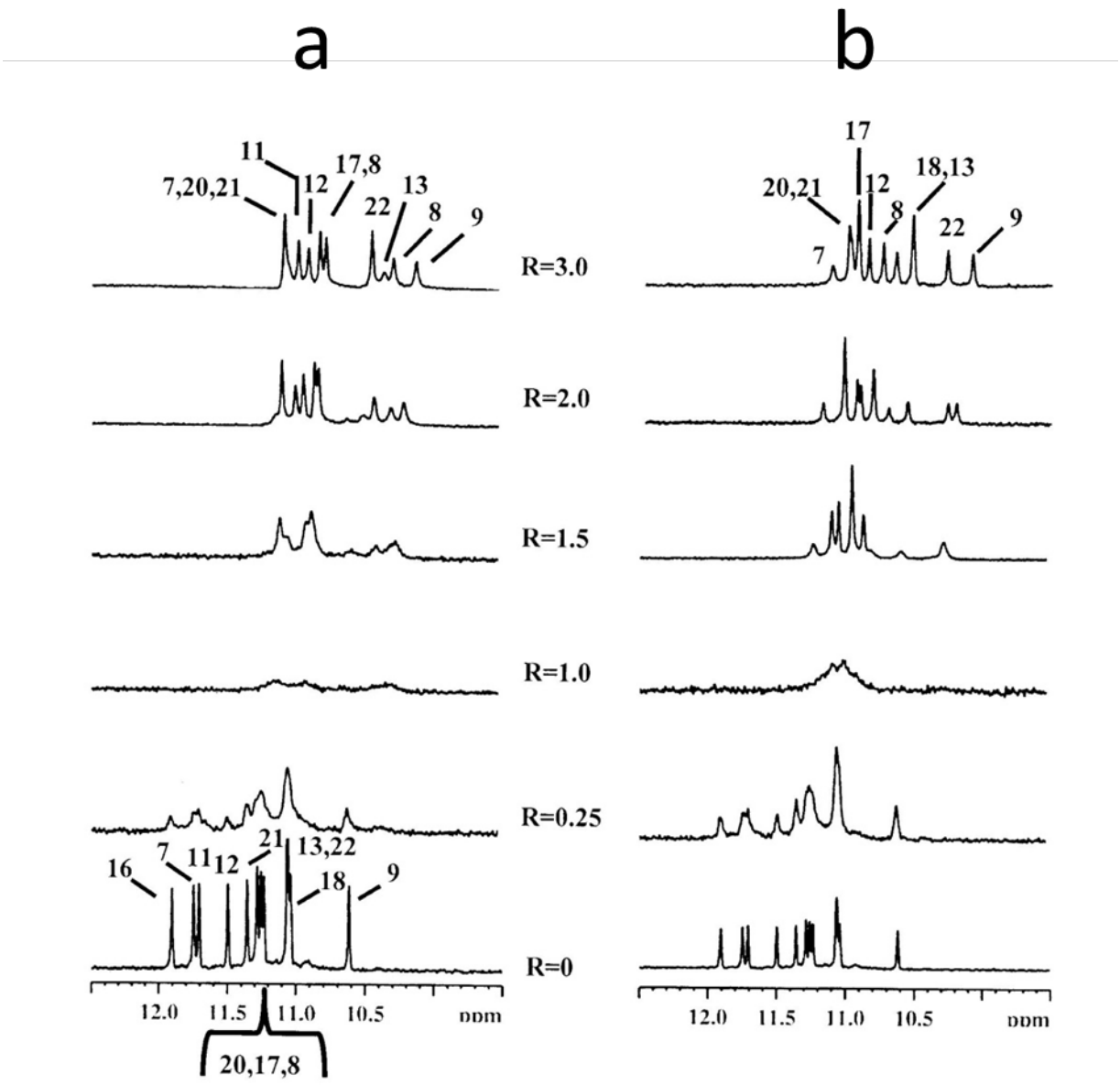

Figure 7. Expanded region of the 2D NOESY spectrum of Pu22-T14T23 / cheleryhthrine complex showing in the boxes: (a) the sequential NOE interactions between the H1 imino protons; (b) and (c) some NOE interactions between the aromatic proton H6 and NCH_3 of chelerythrine and the nucleotide. Experimental conditions are detailed in the main text.

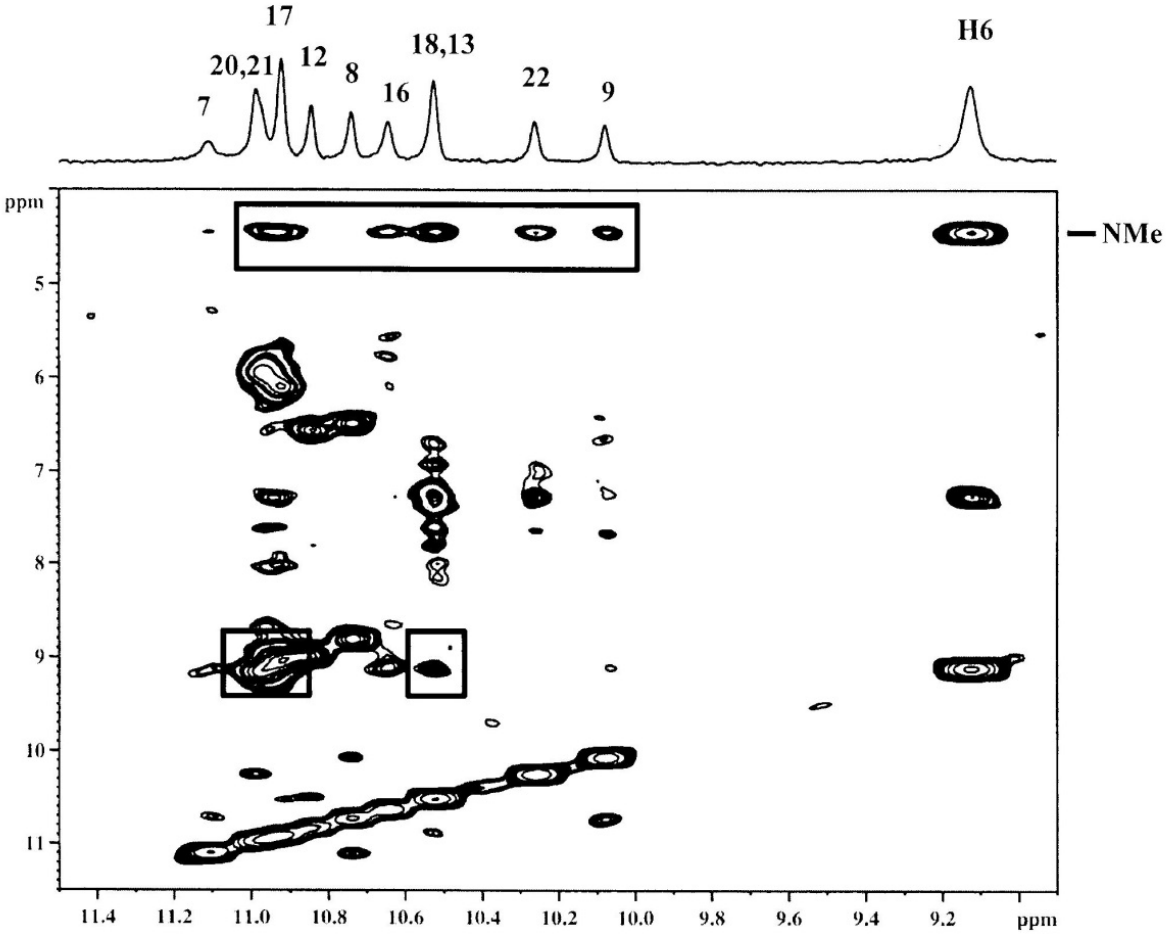

Supplementary Material

Natural quaternary benzo[c]phenanthridine alkaloids selectively stabilize G-quadruplexes

Petra Jarosova [a], Petr Paroulek [a], Michal Rajecky [a], Veronika Rajecka [a], Eva Taborska [b], Ramon Eritja [c], Anna Aviñó [c], Stefania Mazzini [d], Raimundo Gargallo[e], Petr Taborsky*[a]

[a] Faculty of Science, Masaryk University, Kamenice 5, Brno 62500, Czech Republic

[b] Faculty of Medicine, Masaryk University, Kamenice 5, Brno 62500, Czech Republic

[c] Institute for Advanced Chemistry of Catalonia (IQAC-CSIC), CIBER-BBN, Jordi Girona 18-26, E-08034 Barcelona, Spain.

[d] Department of Food, Environmental and Nutritional Sciences (DEFENS), Section of Chemical and Biomolecular Sciences, University of Milan, Via Celoria 2, Milan 20133, Italy;

[e] Department of Chemical Engineering and Analytical Chemistry, University of Barcelona, Martí I Franquès 1-11, 08028 Barcelona, Spain

Contents:

Figure S1. CD spectra of HT22 and ckit21T21 with ligands.

C_{DNA} = 2 μM, C_{QBA} = 4 μM, 10 mM phosphate buffer, 5 mM KCl. Spectra measured at 20°C. All other experimental conditions as detailed in the main text.

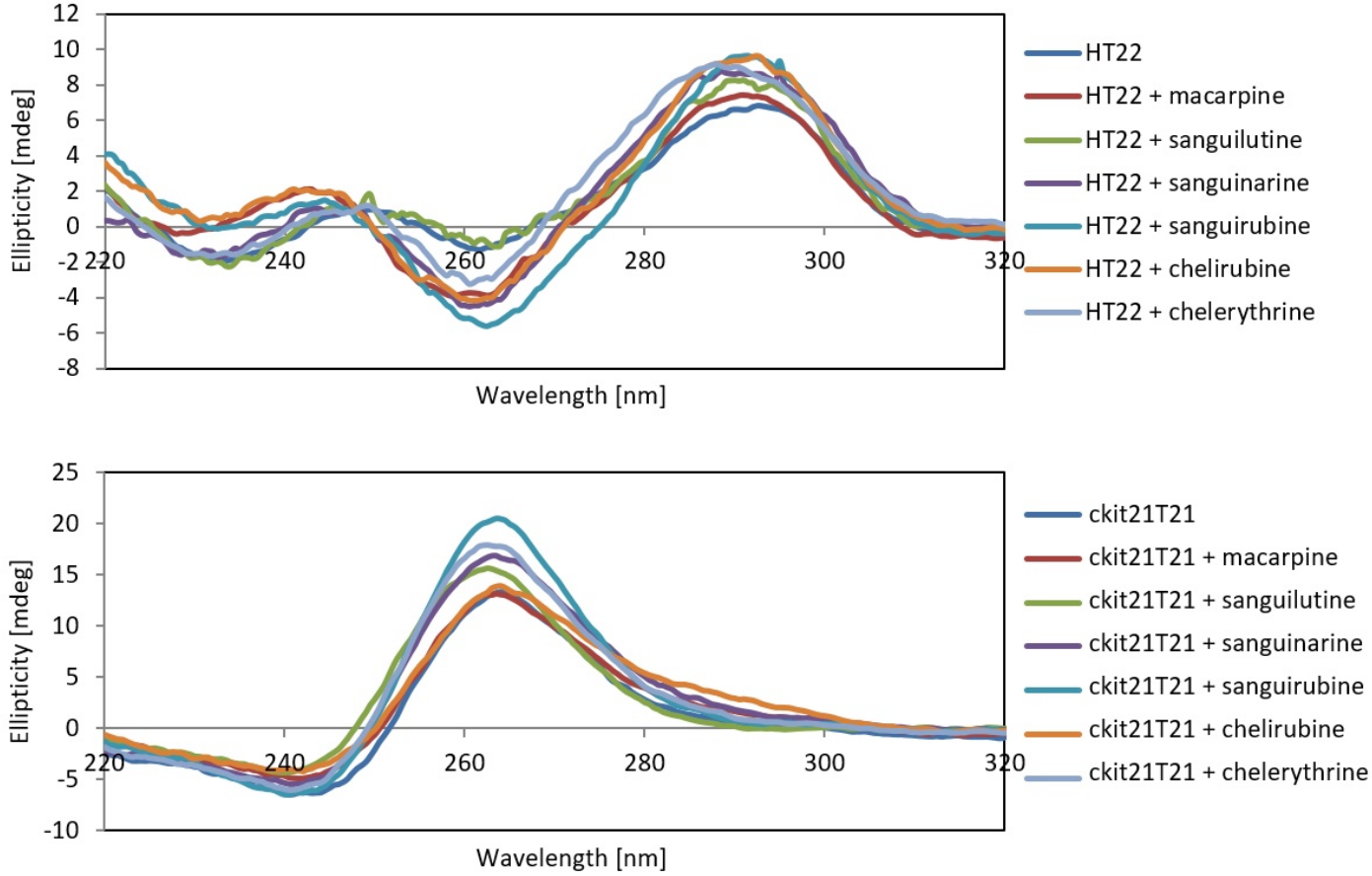

Figure S2. Heating and cooling traces for HT22, ckit21T21 and several QBA:GQ mixtures.

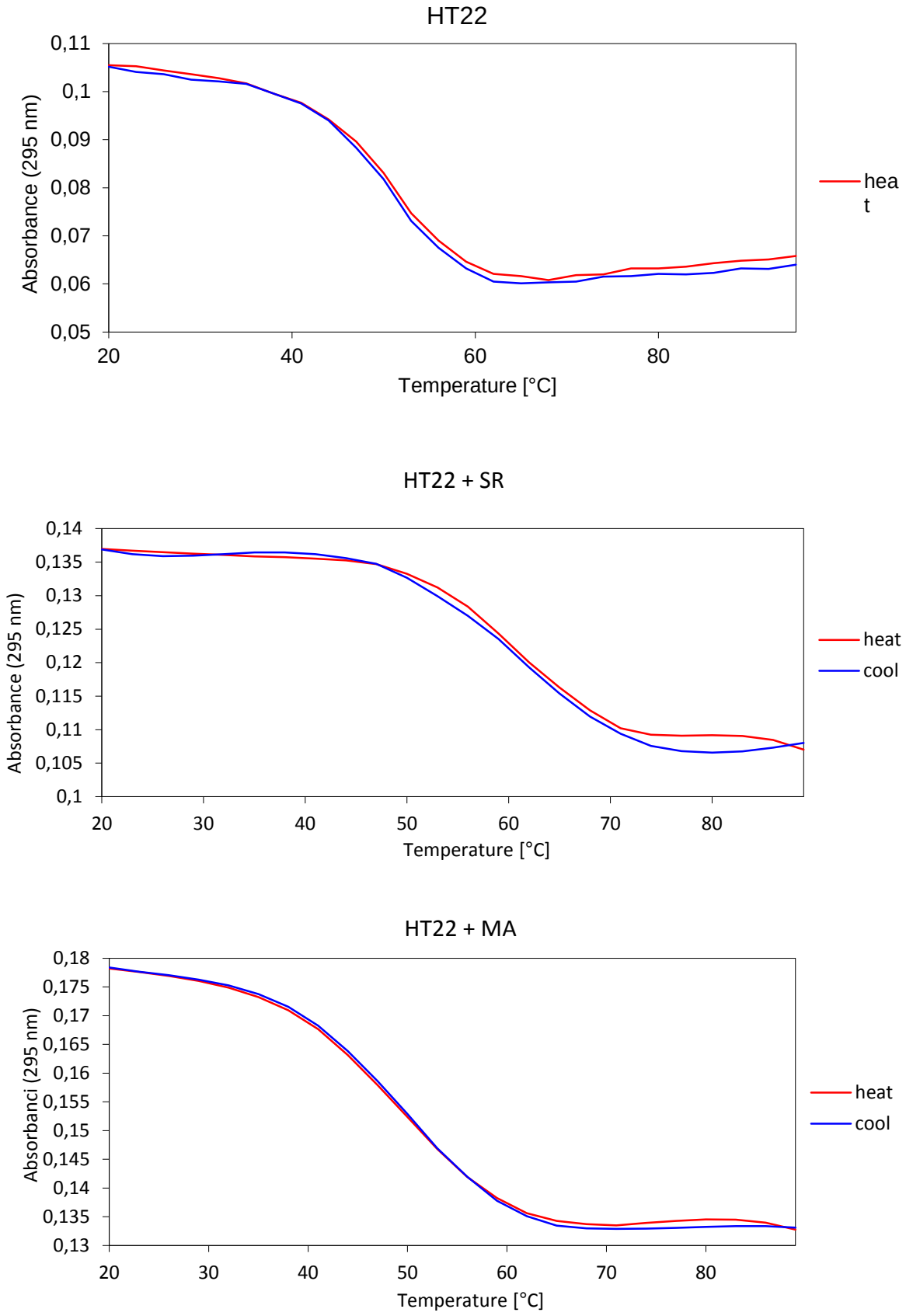

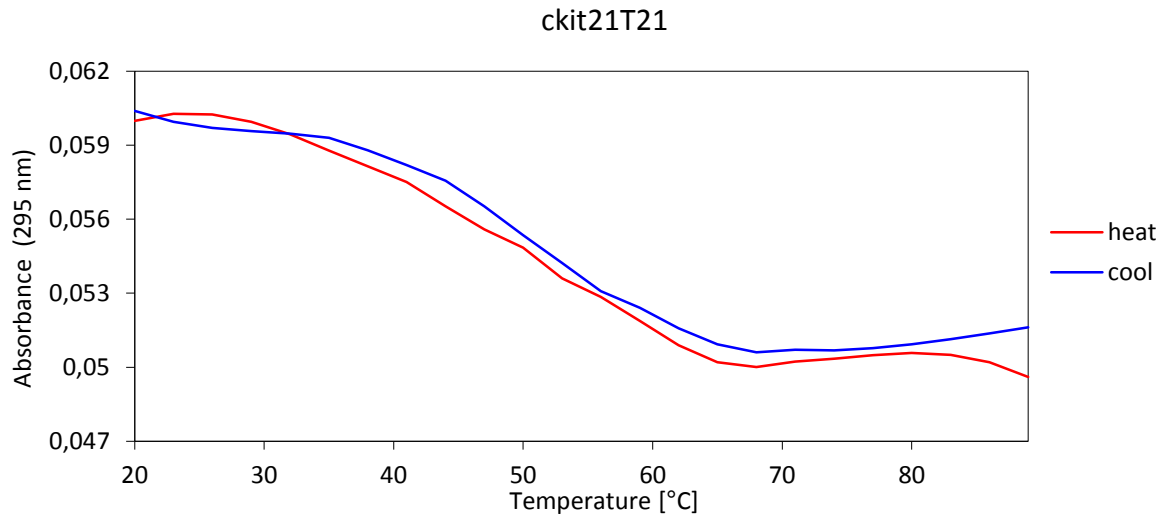
ckit21T21
0,062
0,059
0,056
0,053
0,05
0,047
Absorbance (295 nm)
20
30
40
50
60
70
80
Temperature [°C]
heat
cool

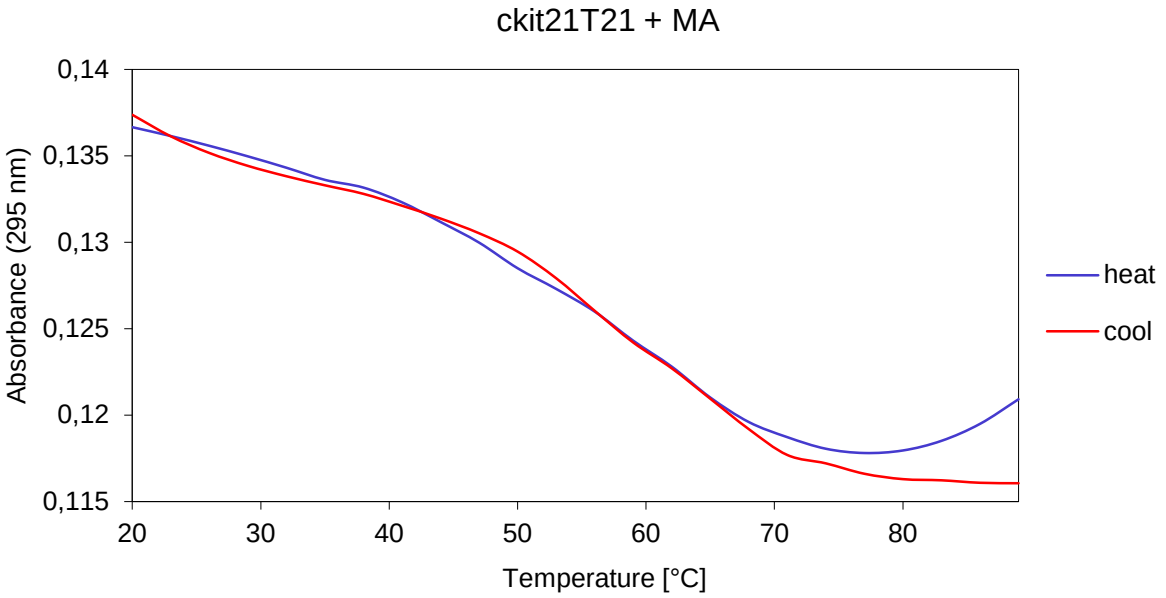
ckit21T21 + MA
0,14
0,135
0,13
0,125
0,12
0,115
Absorbance (295 nm)
20
30
40
50
60
70
80
Temperature [°C]
heat
cool

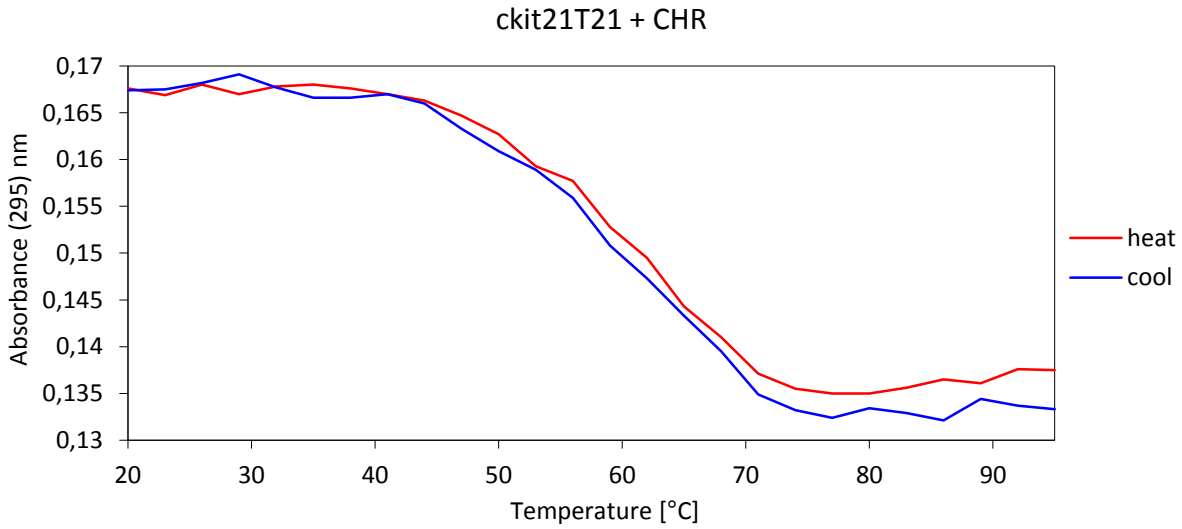
ckit21T21 + CHR
0,17
0,165
0,16
0,155
0,15
0,145
0,14
0,135
0,13
Absorbance (295) nm
20
30
40
50
60
70
80
90
Temperature [°C]
heat
cool

Table S1. [1] H chemical shift values for the complex of sanguilutine with Pu22-T14T23.[a]

	H1/H2/Me	Δδ[b]	H6/H8	Δδ[b]
T4	n.d.	-	n.d.	-
G5	n.d.	-	n.d.	-
A6	n.d.	-	7.95	+0.30
G7	11.04	- 0.72	8.08	+0.08
G8	10.76	- 0.48	7.66	- 0.08
G9	10.10	- 0.55	7.67	- 0.07
T10	n.d.	-	n.d.	-
G11	10.95	- 0.76	n.d.	-
G12	10.90	- 0.60	7.66	-0.02
G13	10.36	- 0.69	7.73	- 0.18
T14	1.98	+0.06	7.68	+0.03
A15	8.38	+0.11	8.57	+0.02
G16	n.d.	-	8.19	+0.08
G17	10.80	- 0.45	7.60	- 0.20
G18	10.28	- 0.74	7.73	- 0.06
T19	2.01	+0.02	7.88	-0.02
G20	11.08	- 0.20	7.85	- 0.04
G21	11.08	- 0.29	7.83	- 0.07
G22	10.43	- 0.61	7.71	-0.10
T23	1.35	- 0.13	6.92	- 0.22
A24	n.d.	-	7.92	+0.15
A25	7.49	+0.10	7.37	-0.13

[a] Measured at 25°C in ppm (δ) from external DSS. Solvent H_2O-D_2O (90:10 v/v), 25 mM phosphate buffer, 70 mM KCl, pH 6.9, R = 3. Other ribose protons showing significant shift variations: T23 H-1'= -0.34. [b] $\Delta\delta = \delta_{bound} - \delta_{free}$.

Table S2. Chemical shift values of chelerythrine in the complex with Pu22-T14T23 and ckit21T12T21.

Chelerythrine	Pu22-T14T23[a]	Δδ[b]	ckit21T12T21[c]	Δδ[b]
H1	6.54	-0.58	6.54	-0.58
2,3 O-CH_2-O	5.91	-0.31	5.91	-0.31
H4	7.27	-0.53	7.30	-0.50
H6	9.11	-0.50	9.20	-0.41
H9	n.d.	-	n.d.	-
H10	n.d.	-	n.d.	-
H11	7.68	-0.42	7.58	-0.52
H12	7.23	-0.57	7.24	-0.56
NCH_3	4.45	-0.45	4.46	-0.54
7-OCH_3	3.90	-0.10	n.d.	-
8-OCH_3	3.90	-0.30	n.d.	-

[a] Measured at 25°C in ppm (δ) from external DSS. Solvent H_2O-D_2O(90:10 v/v), 25 mM phosphate buffer, 70 mM KCl. For Sanguilutine complex aromatic proton H6 and NCH_3 lie at 9.10 ppm and 4.55 ppm respectively. Other aromatic protons were not assigned and lie around 6.8/7.2 ppm. [b] $\Delta\delta = \delta_{bound} - \delta_{free}$. [c] Measured at 25°C in ppm (δ) from external DSS. Solvent H_2O-D_2O (90:10 v/v), 5 mM K-phosphate buffer, 20 mM KCl, pH 6.9.

Table S3. Fluorescence intensity of each QBA:DNA complex– competitive dialysis

	SG (559 nm)	CHE (554 nm)	CHR (596 nm)	MA (589 nm)	SL (593 nm)	SR (591 nm)
Blank	0.9	0.6	0.2	0.3	0.3	0.5
HT22	13.5	10.0	3.7	12.6	14.4	5.7
ckit21T21	**18.1**	15.3	4.3	**17.0**	**19.9**	8.9
T20	2.8	3.0	0.5	2.4	1.0	1.4
ds26	7.0	6.8	2.0	8.6	8.5	4.1
Dickerson	8.5	6.6	2.0	9.9	8.3	2.6

Table S4. Inter-residue NOE interactions of ckit21T12T21 in the complex with chelerythrine. Solvent H_2O-D_2O (90:10 v/v), 5 mM phosphate buffer, 20 mM KCl, pH 6.9, R = 3.

G-tetrad I	*G-tetrad II*	*Tetrad III*
G4H1…..G8H8	G3H1….G7H8	G18H1….G2H8
G8H1…G16H8	G7H1...G15H8	
G16H1…G20H8	G15H1…G19H8	
G20H1…G4H8	G19H1…G3H8	

Table S5. Inter-residue NOE interactions of Pu22-T14T23 in the complexes with sanguilutine and chelerythrine.[a]

G-tetrad I	*G-tetrad II*	*Tetrad III*
G11H1…G16H8	G8H1….G12H8	G9H1….G13H8
G20H1…G7H8	G12H1...G17H8	G13H1…G18H8
G16H1…G20H8[b]	G17H1…G21H8	G18H1…G22H8
G7H1…G11H8[c]	G21H1…G8H8	G22H1…G9H8

[a] Acquired at 25°C in H_2O-D_2O (90:10 v/v), 25 mM phosphate buffer, 70 mM KCl, pH 6.9.

[b] Not detect in sanguilutine complex.

[c] Not detect in chelerythrine complex.

Bibliography

[1] S. Rybakova, M. Rajecky, J. Urbanova, K. Pencikova, E. Taborska, R. Gargallo, P. Taborsky *Chemical Papers*. **2013**, *67*, 568-572.

[2] J. Hammerová, S. Uldrijan, E. Táborská, I. Slaninová *Journal of Dermatological Science*. **2011**, *62*, 22-35.

[3] N. Hatae, E. Fujita, S. Shigenobu, S. Shimoyama, Y. Ishihara, Y. Kurata, T. Choshi, T. Nishiyama, C. Okada, S. Hibino *Bioorganic & Medicinal Chemistry Letters*. **2015**, *25*, 2749-2752.

[4] S. J. Chmura, M. E. Dolan, A. Cha, H. J. Mauceri, D. W. Kufe, R. R. Weichselbaum *Clinical Cancer Research*. **2000**, *6*, 737-742.

[5] A. Das, A. Mukherjee, J. Chakrabarti *Mutation Research-Genetic Toxicology and Environmental Mutagenesis*. **2004**, *563*, 81-87.

[6] T. Ishikawa, T. Saito, H. Ishii *Tetrahedron*. **1995**, *51*, 8447-8458.
[7] H. Sato, R. Yamada, M. Yanagihara, H. Okuzawa, H. Iwata, A. Kurosawa, S. Ichinomiya, R. Suzuki, H. Okabe, T. Yano, T. Kumamoto, N. Suzuki, T. Ishikawa, K. Ueno *Journal of Pharmacological Sciences*. **2012**, *118*, 467-478.
[8] I. Slaninova, Z. Slunska, J. Sinkora, M. Vlkova, E. Taborska *Pharmaceutical Biology*. **2007**, *45*, 131-139.
[9] S. Simeon, J. L. Rios, A. Villar *Pharmazie*. **1989**, *44*, 593-597.
[10] K. Bhadra, G. S. Kumar *Medicinal Research Reviews*. **2011**, *31*, 821-862.
[11] M. Rajecky, I. Slaninova, P. Mokrisova, J. Urbanova, M. Palkovsky, E. Taborska, P. Taborsky *Talanta*. **2013**, *105*, 317-319.
[12] M. Islam, R. Sinha, G. S. Kumar *Biophysical Chemistry*. **2007**, *125*, 508-520.
[13] R. Rodriguez, K. M. Miller *Nature Reviews Genetics*. **2014**, *15*, 783-796.
[14] P. Murat, S. Balasubramanian *Current Opinion in Genetics & Development*. **2014**, *25*, 22-29.
[15] K. W. Lim, S. Amrane, S. Bouaziz, W. X. Xu, Y. G. Mu, D. J. Patel, K. N. Luu, A. T. Phan *Journal of the American Chemical Society*. **2009**, *131*, 4301-4309.
[16] V. Singh, M. Azarkh, T. E. Exner, J. S. Hartig, M. Drescher *Angewandte Chemie-International Edition*. **2009**, *48*, 9728-9730.
[17] Y. Wang, D. J. Patel *Journal of Molecular Biology*. **1993**, *234*, 1171-1183.
[18] G. N. Parkinson, M. P. H. Lee, S. Neidle *Nature*. **2002**, *417*, 876-880.
[19] K. N. Luu, A. T. Phan, V. Kuryavyi, L. Lacroix, D. J. Patel *Journal of the American Chemical Society*. **2006**, *128*, 9963-9970.
[20] K. W. Lim, V. C. M. Ng, N. Martin-Pintado, B. Heddi, A. T. Phan *Nucleic Acids Research*. **2013**, *41*, 10556-10562.
[21] H. Fernando, A. P. Reszka, J. Huppert, S. Ladame, S. Rankin, A. R. Venkitaraman, S. Neidle, S. Balasubramanian *Biochemistry*. **2006**, *45*, 7854-7860.
[22] S. T. D. Hsu, P. Varnai, A. Bugaut, A. P. Reszka, S. Neidle, S. Balasubramanian *Journal of the American Chemical Society*. **2009**, *131*, 13399-13409.
[23] V. Kuryavyi, A. T. Phan, D. J. Patel *Nucleic Acids Research*. **2010**, *38*, 6757-6773.
[24] S. Benabou, R. Eritja, R. Gargallo *ISRN Biochemistry*. **2013**, *2013*, 631875.
[25] S. Benito, A. Ferrer, S. Benabou, A. Aviñó, R. Eritja, R. Gargallo *Spectrochimica Acta Part A: Molecular and Biomolecular Spectroscopy*. **2018**, *196*, 185-195.[26] J. D. Puglisi, I. Tinoco *Methods in Enzymology*. **1989**, *180*, 304-325.
[27] A. Ambrus, D. Chen, J. X. Dai, R. A. Jones, D. Z. Yang *Biochemistry*. **2005**, *44*, 2048-2058.
[28] K. Bhadra, G. S. Kumar *Biochimica Et Biophysica Acta-General Subjects*. **2011**, *1810*, 485-496.
[29] X. H. Ji, H. X. Sun, H. X. Zhou, J. F. Xiang, Y. L. Tang, C. Q. Zhao *Nucleic Acid Therapeutics*. **2012**, *22*, 127-136.
[30] A. R. O. Cousins, D. Ritson, P. Sharma, M. F. G. Stevens, J. E. Moses, M. S. Searle *Chemical Communications*. **2014**, *50*, 15202-15205.
[31] T. Kimura, K. Kawai, M. Fujitsuka, T. Majima *Chemical Communications*. **2006**, 401-402.
[32] T. Yamashita, T. Uno, Y. Ishikawa *Bioorganic & Medicinal Chemistry*. **2005**, *13*, 2423-2430.
[33] L. Scaglioni, R. Mondelli, R. Artali, F. R. Sirtori, S. Mazzini *Biochimica Et Biophysica Acta-General Subjects*. **2016**, *1860*, 1129-1138.
[34] A. Siddiqui-Jain, C. L. Grand, D. J. Bearss, L. H. Hurley *Proceedings of the National Academy of Sciences of the United States of America*. **2002**, *99*, 11593-11598.
[35] J. Dai, T. S. Dexheimer, D. Chen, M. Carver, A. Ambrus, R. A. Jones, D. Yang *Journal of the American Chemical Society*. **2006**, *128*, 1096-1098.
[36] I. Slaninova, J. Slanina, E. Taborska *Chemicke Listy*. **2008**, *102*, 427-433.
[37] J. Urbanova, P. Lubal, I. Slaninova, E. Taborska, P. Taborsky *Analytical and Bioanalytical Chemistry*. **2009**, *394*, 997-1002.
[38] S. Paramasivan, I. Rujan, P. H. Bolton *Methods*. **2007**, *43*, 324-331.
[39] T. R. Wilks, A. Pitto-Barry, N. Kirby, E. Stulz, R. K. O'Reilly *Chemical Communications*. **2014**, *50*, 1338-1340.
[40] K. Wu, S. Y. Liu, Q. Luo, W. B. Hu, X. C. Li, F. Y. Wang, R. H. Zheng, J. Cui, P. J. Sadler, J. F. Xiang, Q. Shi, S. X. Xiong *Inorganic Chemistry*. **2013**, *52*, 11332-11342.
[41] A. Arora, S. Maiti *Journal of Physical Chemistry B*. **2008**, *112*, 8151-8159.
[42] S. Yang, J. F. Xiang, Q. F. Yang, Q. A. Li, Q. J. Zhou, X. F. Zhang, Y. L. Tang, G. Z. Xu *Chinese Journal of Chemistry*. **2010**, *28*, 771-780.
[43] R. Hao, Y. M. Liu, R. G. Zhong *Analytical Methods*. **2014**, *6*, 1059-1066.
[44] F. Doria, A. Oppi, F. Manoli, S. Botti, N. Kandoth, V. Grande, I. Manet, M. Freccero *Chemical Communications*. **2015**, *51*, 9105-9108.
[45] J. X. Dai, M. Carver, L. H. Hurley, D. Z. Yang *Journal of the American Chemical Society*. **2011**, *133*, 17673-17680.

O. Bucket, C.Lin, D. Yang *Science China Chem*. **2014**, 57, 1608-1614.

L. Musso, S. Mazzini, A. Rossini, L.Castagnoli, L. Scaglioni, R. Artali, M. Di Nicola, F. Zunino, S. Dallavalle *Biochimica et Biophysica Acta*. **2018,** 1862, 615–629.